An Experimental and Theoretical Study of the Phase Equilibria in the Fe-Mo-Ni System

KARIN FRISK

New experimental data on the Fe-Mo-Ni phase diagram have been obtained at 1223, 1273, 1373, 1473, and 1543 K using a diffusion couple technique. A number of tie lines were determined using a scanning electron microscope with energy-dispersive X-ray analysis equipment. In a few cases, the phases were identified by X-ray diffraction. The experimental data obtained in the present work, and previously published data, were analyzed by the use of thermodynamic models describing the Gibbs energy of the various phases. The model parameters were calculated using a computerized optimization procedure. The intermetallic phases stable at temperatures above 1223 K were included in the calculations using a three-sublattice model. Experimental data on solidus and liquidus temperatures were used to evaluate properties for the liquid phase. A number of calculated isothermal sections are presented and compared with experimental data. The calculations satisfactorily describe the available experimental data.

I. INTRODUCTION

THE phase equilibria in the Fe-Mo-Ni system have been assessed by Raynor and Rivlin.[1] There are several intermetallic phases in this system. In the Fe-Mo system, the σ, μ, R, and λ phases are present, and in the Mo-Ni system, there are three intermetallic phases, δ, β, and γ. In addition to the intermetallic phases extending from the binary sides, the Fe-Mo-Ni system contains a ternary compound, called the P phase. The approximate compositions of the μ, δ, and P phases are known from previous experimental studies. However, there is some disagreement on the types of equilibria between the different phases, and the extension of the σ and R phases in the ternary system is not known, since the system has not previously been studied at temperatures above 1473 K. The purpose of the present work was to perform a thermodynamic analysis of the Fe-Mo-Ni system, and new information in some parts of the system was needed for a complete analysis. It was therefore decided to first perform an experimental study of the phase equilibria at 1223, 1273, 1373, 1473, and 1543 K using a diffusion couple technique. Measured compositions of phases in equilibrium at different temperatures were thereafter used for the thermodynamic analysis, together with results from previous experimental studies. The analysis of the experimental data involves thermodynamic models describing the Gibbs energy of the individual phases, where the model parameters are determined by a computer optimization procedure. The binary Fe-Mo, Mo-Ni, and Fe-Ni systems have previously been evaluated[2,3,4], and the present study was based upon these assessments. The present description was limited to temperatures above 1223 K, and the λ, β, and γ phases were therefore omitted from the analysis.

KARIN FRISK, formerly with the Division of Physical Metallurgy, Royal Institute of Technology, Stockholm, is with the Swedish Institute for Metals Research, S-114 28 Stockholm, Sweden.

Manuscript submitted July 2, 1990.

II. THE EXPERIMENTAL STUDY

A short description of previous experimental studies on the Fe-Mo-Ni system is given in Section A. The binary systems Fe-Mo, Fe-Ni, and Mo-Ni are seen in Figures 1 through 3. The available experimental data on these binary systems have been assessed and analyzed using thermodynamic models in previous studies. Both phase diagram data and thermochemical data were used. The Fe-Mo system was evaluated by Fernandez-Guillermet,[2] the Mo-Ni system by Frisk,[3] and the Fe-Ni system by Xing *et al.*[4] These assessed binary systems were used in the present study, as a basis for the experimental investigations and for the thermodynamic calculations. The calculated Fe-Mo phase diagram from Reference 2 is shown in Figure 1, the Mo-Ni phase diagram from Reference 3 is shown in Figure 2, and the Fe-Ni phase diagram from Reference 4 is shown in Figure 3. The present experimental study is presented in Section B.

A. *Previous Work*

Raynor and Rivlin[1] assessed the experimental information in the Fe-Mo-Ni system. They discussed the projection of the liquidus surface reported by Köster.[6] We accept their conclusion that the real liquidus surface has no relation to that proposed by Köster and that it therefore would be misleading to try to reproduce their results. For the solid-state equilibria, Raynor and Rivlin also concluded that the results by Köster could not be used. Instead, they relied on more recent data by Das *et al.*[7] and van Loo *et al.*[8] and presented hand-drawn diagrams based upon these data. Das *et al.* investigated the 1473-K isothermal section of the Fe-Mo-Ni system. They examined ternary alloys microscopically, by chemical analysis, and by X-ray diffraction. They found that the μ phase extends approximately half-way across the ternary system and that the P phase is interposed between μ and δ, so that μ and δ do not coexist. They did not determine any equilibria between Mo and the intermetallic phases. Van Loo *et al.*[8] investigated the

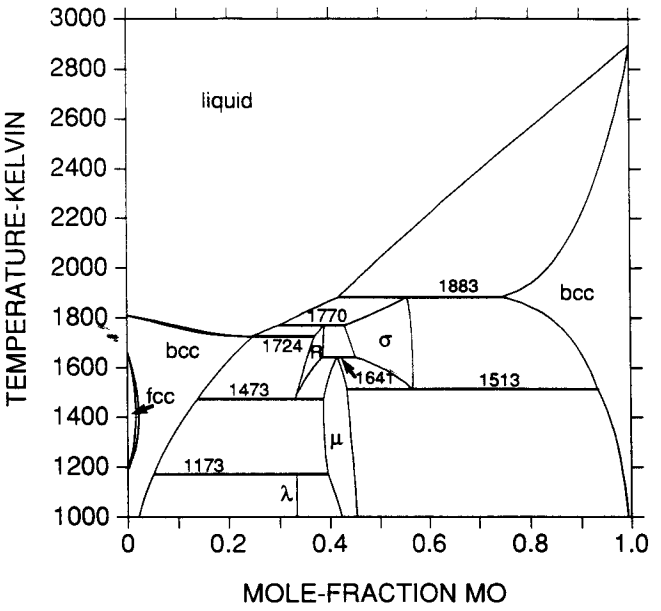

Fig. 1—The calculated Fe-Mo phase diagram according to the thermodynamic evaluation by Fernández Guillermet.[2,13]

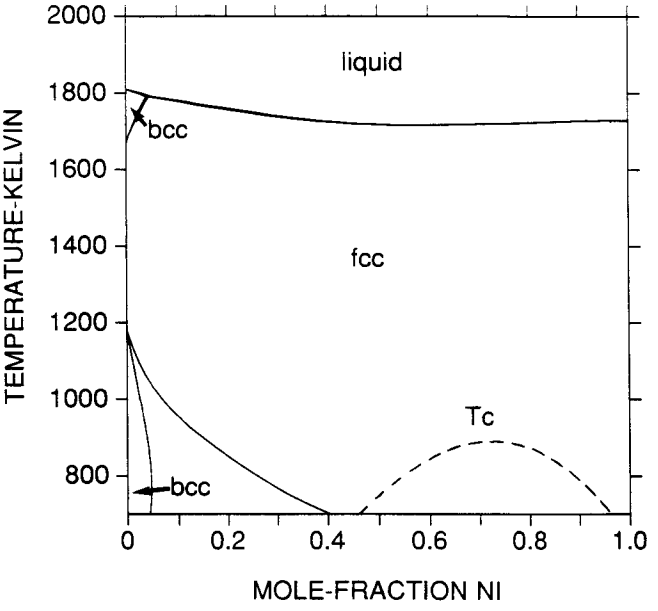

Fig. 3—The calculated Fe-Ni phase diagram according to the thermodynamic evaluation by Xing *et al.*[4]

Fe-Ni-Mo isotherm at 1373 K using a diffusion couple technique and equilibrated ternary alloys. The samples were investigated by use of optical microscopy, microprobe analysis, and X-ray diffraction. They found that the μ phase dissolves 40 at. pct Ni, which is twice as much as Das *et al.* found at 1473 K. In their experimentally determined isothermal section, the *P* phase is not interposed between μ and δ; instead, they found a three-phase equilibrium between μ, δ, and *P*. Gan and Jin[9] recently investigated the isothermal section at 1273 K by a diffusion couple technique, and the compositions of the phases were measured by electron microprobe analysis. They did not find the ternary compound *P* at this temperature. The Fe-Mo-Ni system was also recently studied by Gozlan *et al.*[5] They measured tie lines between the face-centered cubic (fcc) phase and the intermetallic phases and identified the phases by X-ray diffraction at 973, 1123, 1273, and 1473 K. They observed the ternary *P* phase at 1123, 1273, and 1473 K.

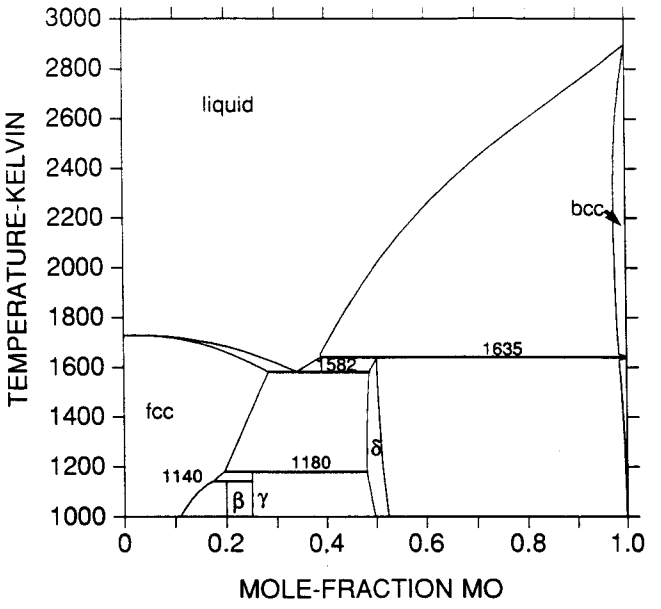

Fig. 2—The calculated Mo-Ni phase diagram according to the thermodynamic evaluation by Frisk.[3]

B. *The Present Work*

1. *Experimental technique*

In the present work, a diffusion couple technique was used. The advantage of such a technique is that an entire isothermal section in a ternary system can be investigated using one sample or few samples. In a first series of experiments, diffusion couple samples were prepared using the pure elements Fe, Mo, and Ni. The compositions of the raw materials are given in Table I. A cylindrical capsule of Fe or Ni, 10 mm in diameter and 20 mm in length with a 3-mm-diameter hole in the center, was filled with discs of Mo and Ni or Fe, 3 mm in diameter and 1 mm in thickness, and closed with a rod of the capsule material. To ensure good contact, the specimen was thereafter compressed parallel to the length axis of the cylindrical capsule. Before the heat treatment, the specimen was sealed in a silica capsule under vacuum. The time and temperatures for the various heat treatments are given in Table II. After heat treatment, the specimen was quenched in brine and the cylinder was cut in half so that the center hole with the metals contained herein were visible. Each part of the diffusion couple can be considered as semi-infinite. The samples were examined by optical microscopy and by scanning electron microscope. The intermetallic phases formed in layers between the different metals. The compositions of the phases were measured using a scanning electron microscope equipped with an energy-dispersive X-ray

Table I. Composition of the Raw Materials Used

Material	Impurity Contents in Weight Percent
Electrolytic iron	0.003 pct Al, <0.01 pct Mn, <0.005 pct S, 0.01 pct C, 0.001 pct Si, 0.003 pct P
Ni (99.98 pct)	<0.01 pct C, <0.0001 pct Al
Mo	0.002 pct W, 0.010 pct Fe, 0.005 pct C, 0.005 pct O, 0.001 pct H, 0.001 pct N

Table II. Heat Treatments of the Diffusion Couples

Capsule	Inset	Temperature (K)	Time (h)
First Series of Experiments Using Pure Fe, Mo, and Ni			
Fe	Ni, Mo	1223	700
Fe	Ni, Mo	1373	100
Fe	Ni, Mo	1473	50
Second Series of Experiments Using Binary Alloys Defined in Table III*			
Fe	alloy C, Mo	1373	97
Ni	alloys D and F	1373	169
Fe	alloy C, Mo	1473	48
Ni	alloy F, Mo	1473	65
Ni	alloy F, Mo	1373	96
Ni	alloy F, Mo	1543	48
Ni	Mo, alloy F, Mo	1373	96
Ni	Mo, alloys F, D, Mo	1543	72
Ni	Mo, alloy F, Mo	1473	72

*The alloys and Mo were inserted in the capsule in the order given under "Inset."

spectrometer (EDS) and LINK AN 10000 X-ray microanalysis system. Measurements were made in several points along a line perpendicular to the phase interfaces, and the compositions of the coexisting phases were evaluated by extrapolating to the position of the interface. Local equilibrium was assumed to hold at the phase boundaries, and the associated compositions were taken as the tie lines. When using pure Fe, Ni, and Mo in the diffusion couple experiments, the layers of the intermetallic phases in some samples were too narrow for measurements across the phase boundaries. Composition measurements using the EDS give a contribution from the surrounding phases if the size of the measured phase is less than approximately 2 μm. A second series of experiments was therefore performed using binary alloys encapsulated in Fe or Ni. The binary alloys were prepared by arc melting of powder compacts and subsequent quenching. The compositions of the powder mixtures were chosen to obtain binary alloys with two-phase structures, bcc (body-centered cubic) + intermetallic or fcc + intermetallic, and with large amounts of intermetallic phase. The actual compositions were not analyzed, but Table III gives the compositions aimed for. The results to be reported will concern compositions of phases in contact with each other, and it is not necessary to know the exact composition of the alloys nor to have homogeneous alloys. The arc-melted binary alloys were cut into discs of 3 mm in diameter and 1 mm in thickness and enclosed in Fe or Ni capsules in the same way as described above. The capsules were heat-treated according to the program given in Table II. The samples were examined by optical and electron microscopy, and the compositions at the phase boundaries were measured, as described above. The binary alloys were found to consist of two-phase structures, as expected. As an example, the microstructure of one such sample, observed by scanning electron microscopy, is shown in Figure 4. In this sample, a binary alloy, "alloy C," was enclosed together with Mo in an Fe capsule and heat-treated at 1373 K for 97 hours. "Alloy C" (38 pct Mo, 62 pct Ni) consists of a two-phase structure, seen in Figure 4. The compositions of the two phases were measured in several regions of the sample, and the measurements show that the dark phase is fcc and the white phase is δ or P phase. The Fe content increases when approaching the Fe-fcc single-phase region (dark region), and a number of tie lines could thus be determined from this sample (seen in the lower part of Figure 10). The lowest Fe content was measured in the center of alloy C, giving the tie line marked by filled circles in Figure 10. From the samples prepared using binary alloys, it was thus possible to cover the entire composition triangle with two to four samples.

To confirm the results from the diffusion couples, some ternary alloys were prepared by arc melting of powder compacts in the same way as described above for binary alloys. The nominal compositions of the powder mixtures are summarized in Table III. The ternary alloys were sealed in silica capsules under vacuum and heat-treated at 1273 and 1373 K for 2 months and at 1473 and 1543 K for 600 hours. The equilibrated alloys were examined in a scanning electron microscope. Two and three phase structures were observed, and the compositions of the phases were measured, as described above. Some of the heat-treated ternary alloys were crushed and analyzed in an X-ray diffractometer to identify the phases (see Section II–B–2).

2. *Experimental results*

The results of the measurements are shown in Figures 5 and 7 through 11 as plotted tie lines, together

Table III. Nominal Compositions of the Various Alloys Used in the Present Work

Binary Alloys		Ternary Alloys	
Composition (At. Pct)	Notation	Composition (At. Pct)	Notation
62 pct Ni 38 pct Mo	alloy C	40 pct Fe 50 pct Mo 10 pct Ni	alloy 1
41 pct Ni 59 pct Mo	alloy D	18 pct Fe 42 pct Mo 40 pct Ni	alloy 2
87 pct Fe 13 pct Mo	alloy E	16 pct Fe 54 pct Mo 30 pct Ni	alloy 3
69 pct Fe 31 pct Mo	alloy F	27 pct Fe 48 pct Mo 25 pct Ni	alloy 4

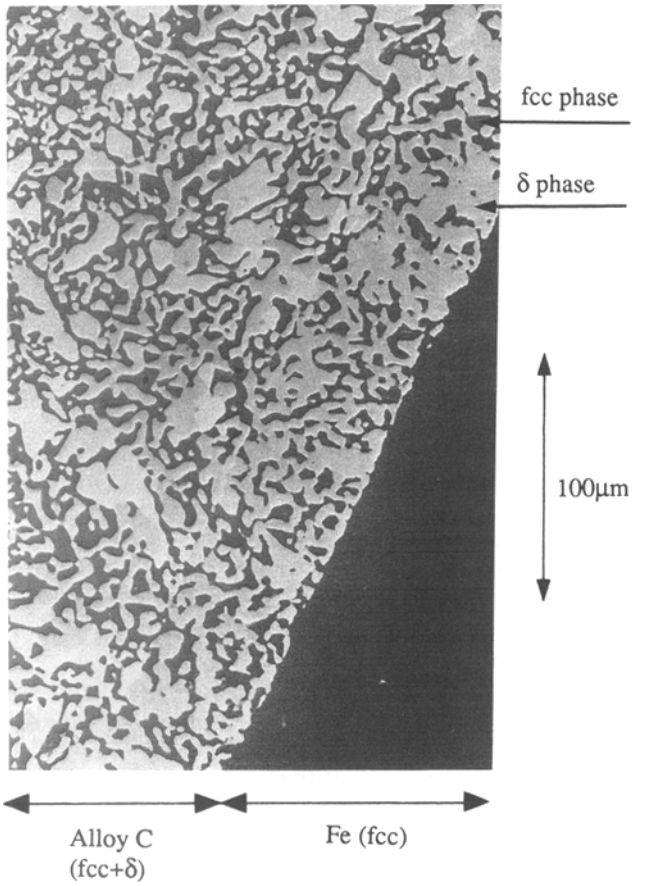

Fig. 4—Example of the microstructure of a diffusion couple sample. This scanning electron picture shows "alloy C" in contact with fcc-Fe. "Alloy C" is composed of two phases, fcc and an intermetallic phase. The Fe content in the two-phase structure increases as the Fe phase region is approached.

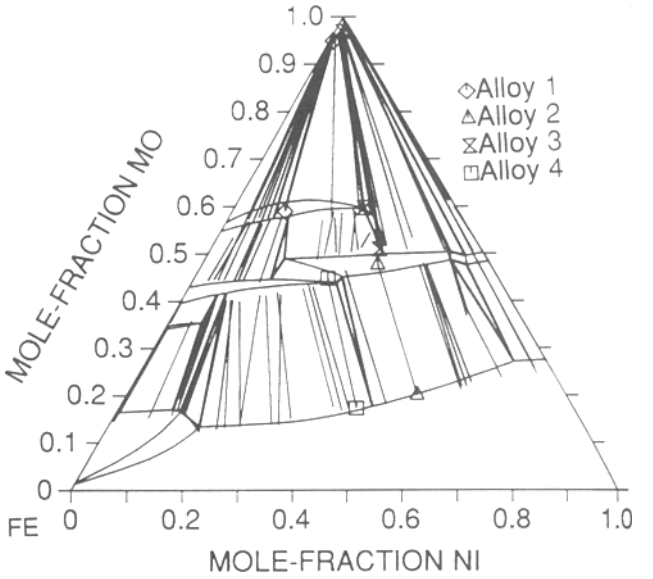

Fig. 5—The calculated isothermal section of the Fe-Mo-Ni system at 1543 K together with experimental data from the present study. The experimental results are plotted as tie lines. The different symbols indicate the end points of the tie lines measured in the equilibrated ternary alloys. These ternary alloys were used for the X-ray diffraction study.

with the results of the calculations described in the following. The results will be discussed for each temperature in Section V. It should be noted that all of the isothermal sections, except the 1223 and 1273 K sections, have been determined from several diffusion couples prepared and heat-treated separately. The experimental tie lines are thus results from independent measurements, and they are in very good agreement. The measurements on the equilibrated ternary alloys, shown in Figures 5, 7, 9, and 11, also confirm the results obtained from the diffusion couples by showing very good agreement with these. The 1223-K section was determined from a single specimen. The layers of the intermetallic phases formed in this specimen were thin, and measurements on these phases was difficult. Therefore, only the compositions of the bcc and fcc phases in equilibrium with the intermetallic phases are reported at this temperature (Figure 13). At 1273 K, only measurements on ternary alloys are reported (Figure 11).

The results of the measurements on diffusion couples at 1543 K are shown in Figure 5 as plotted tie lines. The results from the measurements on ternary alloys are shown in the same figure. In one of the ternary alloys, three phases were present, and the three-phase triangle could be measured. The ternary alloys 1, 3, and 4 (Table III) heat-treated at 1543 K were crushed and examined by X-ray diffraction to identify the phases. It was found that alloy 1 consists of bcc and σ phase, alloy 3 of fcc and P phase, and alloy 4 of fcc and μ phase. The third phase found in alloy 3 was present in such small amounts that is could not be identified by X-ray diffraction. The measured tie lines suggest that it is the σ phase. The phase fraction of σ, P, and μ in these three alloys is high (>80 pct). The results show that the μ phase extends to somewhere between 24 and 32 at. pct of Ni at approximately constant Mo contents and is followed by the P phase. Since the μ and P phases lie very close in composition, it was difficult to distinguish between the two phases by tie line measurements only. Further, the X-ray diffraction results confirmed that the phase extending into the system at high Mo contents is the σ phase. If the results of the measurements on ternary alloys heat-treated at different temperatures are compared, we see that alloy 4 gives $\gamma + \mu$ at 1543 K, Mo + P at 1473 K, single-phase μ (or P) at 1373 K, and Mo + μ (or P) at 1273 K. This change of equilibrium suggests that there is a shift of the μ and P phases toward lower Mo contents with decreasing temperatures. However, there is also a slight variation of the overall composition of the alloys between the different samples.

III. THERMODYNAMIC MODELS

A. *Model for the Bcc, Fcc, and Liquid Phases*

The bcc, fcc, and liquid phases were described by the following model:

$$G_m = x_{Fe}{}^{\circ}G_{Fe} + x_{Mo}{}^{\circ}G_{Mo} + x_{Ni}{}^{\circ}G_{Ni} + RT(x_{Fe} \ln x_{Fe} + x_{Mo} \ln x_{Mo} + x_{Ni} \ln x_{Ni}) + {}^{E}G_m + G_m^{mg} \quad [1]$$

The $^{\circ}G$ parameters represent the Gibbs energy of the elements in a hypothetical nonmagnetic state and are taken from previous assessments of Fe[10], Mo[11], and Ni.[12] The $^{\circ}G$ parameters are referred to the enthalpy of the stable state at 298.15 K and 0.1 MPa. The term $^{E}G_m$ represents the excess Gibbs energy and is given by

$$^{E}G_m = x_{Fe}x_{Mo}L_{Fe,Mo} + x_{Fe}x_{Ni}L_{Fe,Ni} + x_{Mo}x_{Ni}L_{Mo,Ni} + x_{Fe}x_{Mo}x_{Ni}L_{Fe,Mo,Ni} \quad [2]$$

The parameters denoted L represent interactions between the elements. They can be composition dependent according to

$$L_{A,B} = \sum_{i=0} {}^{i}L_{A,B}(x_A - x_B)^i \quad [3]$$

All L parameters representing interactions between two elements are taken from previous assessments of the Fe-Mo[2], Mo-Ni[3], and Fe-Ni[4] systems. The ternary term is evaluated in the present work for the bcc, fcc, and liquid phases. For the fcc phase, the ternary parameter was given the following composition dependence:

$$L_{Fe,Mo,Ni} = x_{Fe}{}^{\circ}L_{Fe} + x_{Mo}{}^{\circ}L_{Mo} + x_{Ni}{}^{\circ}L_{Ni} \quad [4]$$

B. *Models for the Intermetallic Phases*

1. *Previous work*

As mentioned above, seven intermetallic phases are present in the Fe-Mo-Ni system, σ, μ, R, λ, P, δ, β, and γ, where the P phase is a ternary phase, and the remaining phases are extensions from the binary sides of the diagram (from the Fe-Mo and Ni-Mo systems). The σ, μ, R, and λ phases are stable in the Fe-Mo system. They were studied by Fernández Guillermet in his evaluation of the Fe-Mo system.[13] Fernández Guillermet gave a detailed description of how the crystal structure of the intermetallic phases in the Fe-Mo system can be taken into account in modeling the phases.[13] A revised version[2] of the Fe-Mo system was used in the present work with a slightly modified model for the σ phase. That Fe-Mo phase diagram is shown in Figure 1, and the revised parameter values are given in the Appendix. The atoms in the intermetallic phases are divided on sites with different coordination numbers, and different types of atoms prefer different sites. Only four different coordination environments are allowed, with coordination numbers 12, 14, 15, and 16 (denoted CN12, CN14, CN15, and CN16). To model this, a sublattice model was used,[14,15] and the number of sublattices was, for practical reasons, reduced to 3. The distribution of the elements on the different sublattices was chosen by taking into account experimental data, if such are available, or by making reasonable guesses, based on, for example, atomic sizes. The δ phase in the Mo-Ni system was modeled using the same procedure as used by Fernández Guillermet for the Fe-Mo system. The λ (Fe-Mo), β, and γ (Mo-Ni) phases were not included in the present study. To model the intermetallic phases in the ternary Fe-Mo-Ni system, the results from the binary assessments were used, and a choice was made of how to place the third element on the different sublattices. For the case of the P phase that is not stable in the binary systems, a model was chosen based on ternary information. The

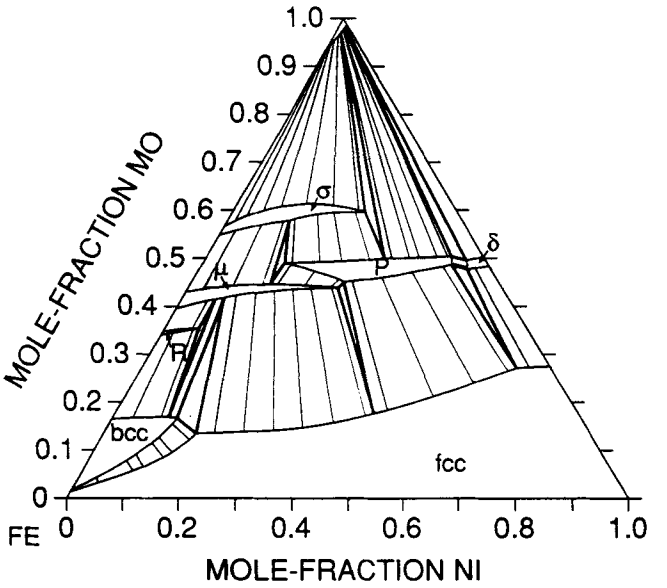

Fig. 6—The calculated isothermal section at 1543 K. The tie lines are calculated.

models chosen for each intermetallic phase are summarized in Table IV, and they are discussed in the following section. Similar three-sublattice descriptions of intermetallic phases have previously been successful in the evaluations of ternary systems.[16–19]

2. *The models for the intermetallic phases*

The σ phase:

The sigma phase is stable in the Fe-Mo system at temperatures above 1513 K[2] (Figure 1). In the present experimental study, it was found that the σ phase extends into the ternary system at the highest investigated

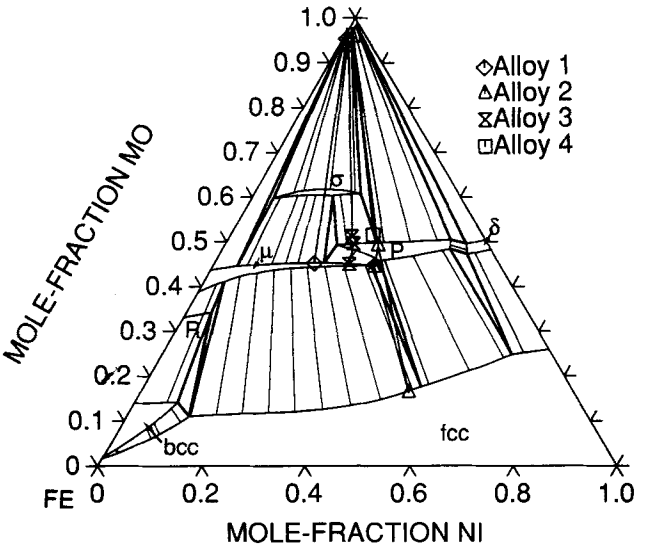

Fig. 7—The calculated isothermal section at 1473 K. The tie lines are calculated. The σ phase is present in this calculation although it has not been found experimentally at this temperature. The different symbols indicate the end points of the tie lines measured in the equilibrated ternary alloys in the present work.

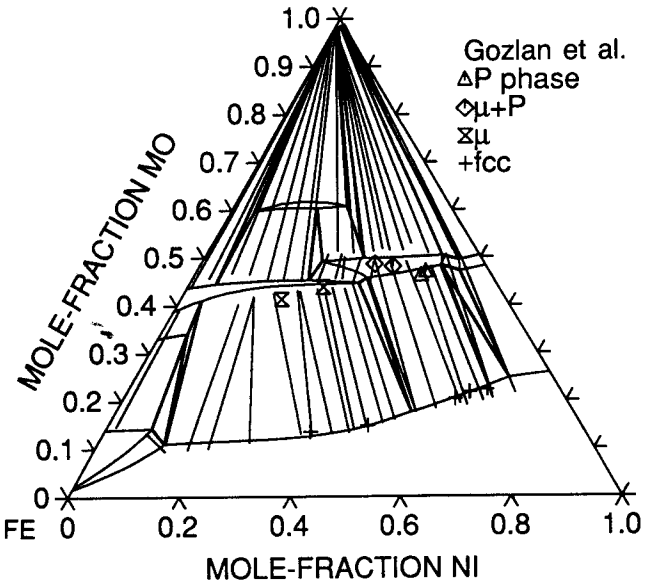

Fig. 8—The calculated isothermal section at 1473 K, together with experimental tie lines from the present study and from Ref. 5. The σ phase is present in the calculated section although it has not been found experimentally at this temperature.

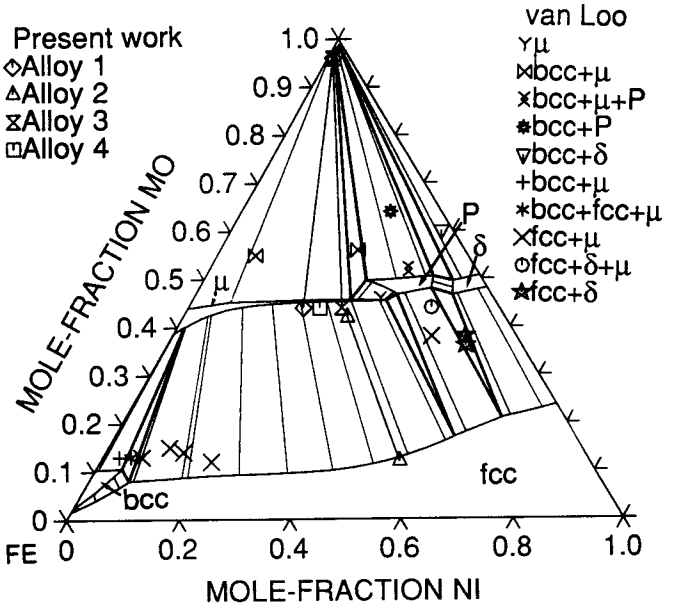

Fig. 9—The calculated isothermal section at 1373 K together with experimental data from the present work and by van Loo *et al.*[8] The tie lines are calculated, except those marked by symbols which were measured in the present work, on equilibrated ternary alloys.

temperature (1543 K), along a line of approximately constant Mo content. The binary model for the σ phase was thus extended by placing the Ni aoms on the same sublattices as Fe.

The μ phase:

The μ phase is found over a large temperature range in the Fe-Mo system, and it was found in all of the sections investigated in the present work, extending into the ternary system with an approximately constant Mo content. The μ phase was thus modeled so that Ni substitutes for Fe, using the model from the binary Fe-Mo system.

The R phase:

The *R* phase is stable in the Fe-Mo system at high temperatures. At the highest temperature investigated in the present work (1543 K), the *R* phase was found to dissolve about 5 at. pct Ni. It was therefore assumed that Ni goes into the same sublattices as Fe.

The δ phase

Sinha[20] has reviewed data on the topological close-packed structures of the transition metal alloys and data on the δ phase. The distribution of the Ni and Mo atoms on the different sites has been measured, and these data were used for modeling the δ phase in the Mo-Ni system. There are no such data for the distribution of Fe. In the present experimental work and in the studies by Das *et al.*[7] and van Loo *et al.*,[8] it was found that the solubility of Fe in δ lies between 3 and 5 pct. To be able to account for this information, it is necessary to make an assumption on how the Fe atoms are ordered on the sites, and we chose to let the Fe atoms occupy the same sites as the Ni atoms.

The P phase:

Sinha[20] reviewed data on the *P* phase, first discovered in the Cr-Ni-Mo system.[21] However, he did not mention its existence in the Fe-Mo-Ni system. Das *et al.*[7] reported a ternary phase in the Fe-Mo-Ni system isomorphous with the Cr-Mo-Ni ternary *P* phase. According to the compilation of Sinha,[20] there are 56 atoms in the unit cell divided on sites with different coordination numbers. The occupancy of the atoms on the different sites is known in the Cr-Mo-Ni system. The Mo atoms occupy the sites with the highest coordination numbers, and Mo was thus placed on sublattices 2 and 3. Nickel occupies the CN12 sites and was placed on the first sublattice, but also on the second to be able to account for

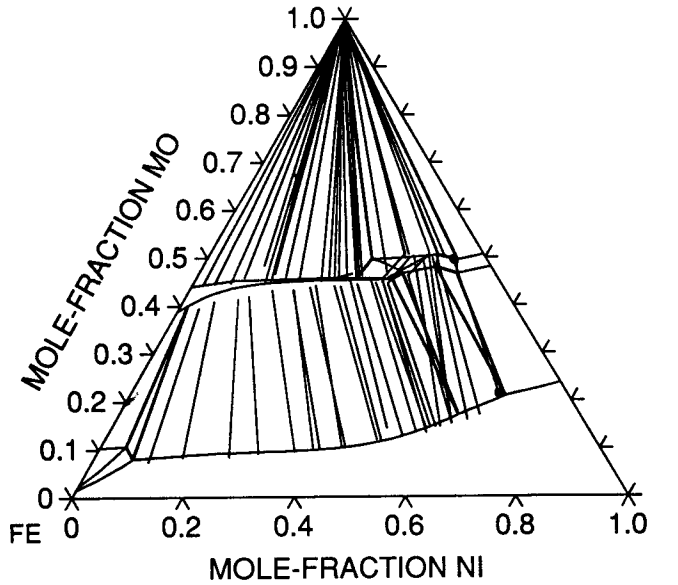

Fig. 10—The calculated isothermal section 1373 K together with experimental data from the present study. The experimental results are plotted as tie lines. The tie line marked with filled circles was measured in the sample shown in Fig. 4.

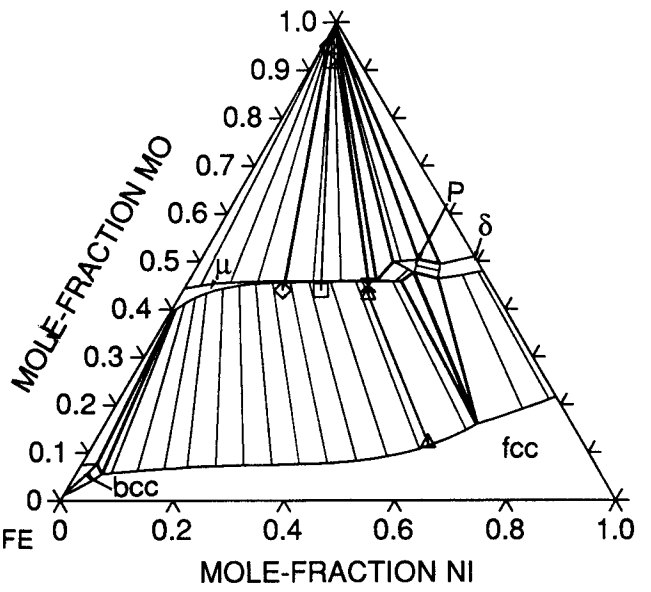

Fig. 11—The calculated isothermal section at 1273 K together with experimental data from the present study. All tie lines are calculated, except those marked with symbols which are tie lines measured in the present study, on ternary equilibrated alloys.

the experimental results of the present study that show that the *P* phase has varying Mo content at 1543 K. Iron was placed on the same sublattices as Ni. We thus get the model listed in Table IV.

3. *The Gibbs energy*

All the intermetallic phases are described with a model of the type

$$(\mathrm{Fe, Ni})_a(\mathrm{Fe, Mo, Ni})_b(\mathrm{Mo})_c$$

where a, b, and c are the number of sites on each sublattice. For one formula unit of this type, the sublattice model[14,15] yields an expression of the Gibbs energy of each phase as follows:

$$\begin{aligned} G_m = {}& {}^1y_{\mathrm{Fe}}({}^2y_{\mathrm{Fe}}{}^\circ G_{\mathrm{Fe:Fe:Mo}} \\ & + {}^2y_{\mathrm{Mo}}{}^\circ G_{\mathrm{Fe:Mo:Mo}} + {}^2y_{\mathrm{Ni}}{}^\circ G_{\mathrm{Fe:Ni:Mo}}) \\ & + {}^1y_{\mathrm{Ni}}({}^2y_{\mathrm{Fe}}{}^\circ G_{\mathrm{Ni:Fe:Mo}} \\ & + {}^2y_{\mathrm{Mo}}{}^\circ G_{\mathrm{Ni:Mo:Mo}} + {}^2y_{\mathrm{Ni}}{}^\circ G_{\mathrm{Ni:Ni:Mo}}) \\ & + aRT({}^1y_{\mathrm{Fe}} \ln {}^1y_{\mathrm{Fe}} + {}^1y_{\mathrm{Ni}} \ln {}^1y_{\mathrm{Ni}}) \\ & + bRT({}^2y_{\mathrm{Fe}} \ln {}^2y_{\mathrm{Fe}} + {}^2y_{\mathrm{Mo}} \ln {}^2y_{\mathrm{Mo}} \\ & + {}^2y_{\mathrm{Ni}} \ln {}^2y_{\mathrm{Ni}}) + {}^E G_m \end{aligned} \quad [5]$$

Table IV. The Models Used for the Intermetallic Phases of the Fe-Mo-Ni System

Phase	Model
σ	$(\mathrm{Fe, Ni})_8(\mathrm{Fe, Ni, Mo})_{18}(\mathrm{Mo})_4$
μ	$(\mathrm{Fe, Ni})_7(\mathrm{Fe, Ni, Mo})_4(\mathrm{Mo})_2$
R	$(\mathrm{Fe, Ni})_{27}(\mathrm{Fe, Ni, Mo})_{12}(\mathrm{Mo})_{14}$
δ	$(\mathrm{Fe, Ni})_{24}(\mathrm{Fe, Ni, Mo})_{20}(\mathrm{Mo})_{12}$
P	$(\mathrm{Fe, Ni})_{24}(\mathrm{Fe, Ni, Mo})_{20}(\mathrm{Mo})_{12}$

where ${}^E G_m$ is the excess Gibbs energy. The term ${}^i y_{\mathrm{M}}$ denotes the fraction of M (where M is Fe, Ni, or Mo) on the sublattice i (i is the sublattice 1 or 2, where there is mixing of atoms). The term ${}^\circ G_{\mathrm{Fe:Ni:Mo}}$, as an example, represents the Gibbs energy of the phase in question with Fe on the first sublattice, Ni on the second sublattice, and Mo on the third sublattice, and similarly for the other ${}^\circ G$ parameters. The ${}^\circ G$ parameters were referred to the selected standard states of the pure elements. Some ${}^\circ G$ parameters are given from previous evaluations of binary and ternary systems.[2,3,22] Since the available information for the evaluation of the remaining ${}^\circ G$ parameters is very limited, a simplification was introduced. Andersson *et al.*[23] suggested that the ${}^\circ G$ parameters can be estimated by comparing the elements on the different sublattices with the values for the elements in the bcc or fcc state. An element on a sublattice with a coordination number of 12 is compared with the fcc state of the element, and an element on sublattices with a coordination number of 14 or higher is compared with the bcc state of the element. Using this suggestion, the elements on the first sublattice are compared with fcc and on the two second sublattices (CN14, CN15, or CN16) are compared with the bcc state. For our example above, we thus get

$${}^\circ G_{\mathrm{Fe:Ni:Mo}} = a{}^\circ G^{\mathrm{fcc}}_{\mathrm{Fe}} + b{}^\circ G^{\mathrm{bcc}}_{\mathrm{Ni}} + c{}^\circ G^{\mathrm{bcc}}_{\mathrm{Mo}} + \Delta{}^\circ G_{\mathrm{Fe:Ni:Mo}} \quad [6]$$

and similarly for all other ${}^\circ G$ parameters (Appendix). The term $\Delta{}^\circ G_{\mathrm{Fe:Ni:Mo}}$ is a correction term that is evaluated from experimental data.

The excess Gibbs energy was in the present work, for simplicity, set to zero for all phases except the σ phase. For the σ phase, it was given the following expression:

$${}^E G = {}^1y_{\mathrm{Fe}}{}^2y_{\mathrm{Fe}}{}^2y_{\mathrm{Mo}} L_{\mathrm{Fe:Fe,Mo:Mo}} + {}^1y_{\mathrm{Fe}}{}^1y_{\mathrm{Ni}}{}^2y_{\mathrm{Mo}} L_{\mathrm{Fe,Ni:Mo:Mo}} \quad [7]$$

where $L_{\mathrm{Fe:Fe,Mo:Mo}}$ is taken from Reference 2 and $L_{\mathrm{Fe,Ni:Mo:Mo}}$ was determined in the present work.

IV. PARAMETER EVALUATION

A. *The Solid Phases*

The experimental data obtained in the present work, as well as previously published experimental data, were taken into account for the evaluation of the thermodynamic parameters. A set of experimental data was selected for each temperature. Each piece of information was given a weight chosen by personal judgement. The weight should reflect the experimental uncertainty. The weighted set of data was analyzed using the thermodynamic models described above. The model parameters were evaluated using a computer optimization program[25] which minimizes the weighted sum of squared deviations between calculated values and experimentally determined values. Different choices of weights and different sets of parameters were tried until most of the data were reproduced within the expected uncertainty limits.

Since all phases are present at 1543 K, this temperature was first considered in the optimization. At this temperature, we know from the present investigation of

ternary alloys that the μ phase extends to over 25 at. pct Ni, and that it is followed by the P phase at approximately 30 at. pct Ni. The three-phase equilibria bcc + fcc + μ, bcc + R + μ, and σ + P + bcc were measured in diffusion couple samples. The extension of the δ phase at this temperature is not known, but we know from the data at lower temperatures that it should solve around 5 at. pct Fe. The equilibria between the fcc, P, δ, and μ phases were first fixed. A number of correction terms, defined above, were evaluated for the different phases. For the P phase that has not been evaluated in any of the binary systems, four binary and two ternary $^{\circ}G$ parameters were evaluated. The μ phase is stable in the Fe-Mo system, and the parameters for the binary μ phase have been determined previously.[13] The two binary $^{\circ}G$ parameters on the Ni-Mo side were evaluated, as well as two ternary parameters. The parameters for the δ phase in the Mo-Ni system were taken from a previous study.[3] The δ-phase parameters in the Fe-Mo binary, representing very unstable states, were given a high positive value. The correction terms for the ternary δ-phase parameters were set to zero. To describe the measured fcc + intermetallic phase boundary, three ternary composition-dependent parameters in the fcc phase were evaluated, and a ternary interaction parameter was evaluated in the bcc phase to describe the measured bcc + fcc phase equilibria. The bcc + R + μ three-phase triangle was measured at 1543 K, and this result was used to evaluate the parameters for the R phase on the Mo-Ni side. The correction terms for the ternary parameters were set to zero for the R phase. The σ phase is stable in the Fe-Mo system at 1543 K (Figure 1). It therefore appears in the 1543-K isothermal section of the Fe-Mo-Ni system. In the ternary alloy 3, a three-phase equilibria was measured, probably between the σ, P, and bcc phases. X-ray diffraction investigation of the ternary alloy 1 heat-treated at 1543 K confirmed that the σ phase was present (Figure 5). The σ-phase parameters were therefore evaluated to fit a solubility of Ni in the σ phase of 23 at. pct. The Cr-Mo-Ni system was evaluated in connection to the present work, and the σ phase is a dominating ternary compound in that system.[22] We therefore chose to determine the binary Mo-Ni parameters for the σ phase using the ternary Cr-Mo-Ni data, instead of the Fe-Mo-Ni data. All binary parameters for the σ phase are then fixed, and the ternary $^{\circ}G$ parameters must be given a large positive value to reduce the existence range of the σ phase. An interaction parameter $L_{Fe,Ni:Mo:Mo}$ was evaluated to fit the compositions measured in the present work. All parameters describing the Fe-Mo-Ni system are listed in the Appendix. The calculated isothermal section at 1543 K using these parameters is shown in Figures 5 and 6 together with experimental data.

The experimental data from temperatures lower than 1543 K were used to evaluate the temperature dependence of the various parameters. The best data are those at 1473 and 1373 K, and only these were used for the parameter evaluation. The experimental data from the present work, in agreement with results by Gozlan *et al.*[5] at 1473 K and with van Loo *et al.*[8] at 1373 K, show that the μ phase extends to higher Ni contents and the extension of the P phase decreases as the temperature is lowered. There is a small disagreement on the position of the fcc + μ + P three-phase equilibrium between the present work and previous investigations.[5,8] The data from the present work were selected since the results at different temperatures are consistent, and the entire composition triangles have been determined. The experimental data permitted an evaluation of the temperature dependence of a number of the correction terms for the μ and P phase. The σ phase has not been found at temperatures below 1543 K, and the temperature dependencies for the σ phase were set to values of the same order of magnitude as for the μ and P phases. All evaluated parameters are listed in the Appendix.

B. *The Liquid Phase*

Bamberger *et al.*[26] measured the liquidus and solidus temperature of some ternary alloys. The measured liquidus temperatures were used to evaluate a ternary interaction parameter in the liquid phase. The measured and calculated temperatures are shown in Table V, and the liquidus temperatures are in reasonable agreement. No attempt was made to improve the agreement with measured solidus temperatures. This would involve a reoptimization of the fcc phase parameters, and it was felt that they are well determined from the experimental data on the fcc/fcc + intermetallic phase boundary.

V. DISCUSSION

The calculated isothermal section at 1543 K is shown in Figures 5 and 6. The agreement with experimental data is very good. The calculated bcc + fcc + μ, bcc + R + μ, and bcc + σ + P three-phase equilibria lie almost exactly over the measured equilibria. The calculated 1473 K section is shown in Figure 7, together with experimental results from the equilibrated ternary alloys. The calculated isothermal section (Figures 7 and 8) agrees well with the experimentally determined

Table V. Comparison between Measured[26] and Calculated Liquidus and Solidus Temperatures

Alloy Composition (Wt Pct)			Measured Solidus	Calculated Solidus	Measured Liquidus	Calculated Liquidus
Pct Fe	Pct Ni	Pct Mo				
10	56	34	1589	1637	1633	1642
13.1	54.1	32.84	1588	1639	1628	1641
16.2	52.16	31.67	1587	1639	1631	1639
20.38	49.54	30.08	1587	1636	1632	1637
31.14	42.85	26.02	1593	1630	1640	1630
41.84	36.19	21.98	1598	1630	1656	1632

section, except for the occurrence of the σ phase. Although it has not been found experimentally, the calculations predict the σ phase to be stable at this temperature. Alloy 1, equilibrated at 1473 K for 600 hours, did not contain σ phase (Figure 7). Nor was the σ phase detected in the diffusion couple experiments (Figure 8). In the calculations, the σ phase is stable at 1473 K and disappears at 1400 K. There is thus an error in the calculated range of stability of the σ phase of approximately 100 K. Unreasonably high temperature dependencies of the ternary correction terms for the σ phase are needed to correct this error if we also use the experimental results from 1543 K and the parameters evaluated in the Cr-Mo-Ni system.[22] The calculated result shown in Figures 7 and 8 is the best that could be done under the circumstances and was accepted for the present purpose.

In Figure 8, the 1473-K section is compared with experimental data from the present work and from Gozlan *et al.*,[5] who identified the phases by X-ray diffraction. The agreement is again good. At this temperature, the equilibrium between the fcc, δ, and P phases was measured, and it is reasonably well described. The calculated isothermal section at 1373 K is shown in Figure 9, together with experimental data from the present work and from van Loo *et al.*[8] The agreement is good except for the existence range of the P phase. Van Loo *et al.*[8] found that the μ, δ, and P phases are in equilibrium at this temperature. In the present description, this three-phase equilibrium appears first at lower temperatures. In Figure 10, the calculated section at 1373 K is compared with experimental results obtained in the present work from diffusion couples. The agreement is reasonable. The experiments indicate that the P phase should have a slightly more narrow existence range. The experiments at 1473 K (Figure 7) lead to the same conclusion. The present calculation was accepted, since a change of the existence range of the P phase affects the fcc/fcc + P phase boundary, giving less good

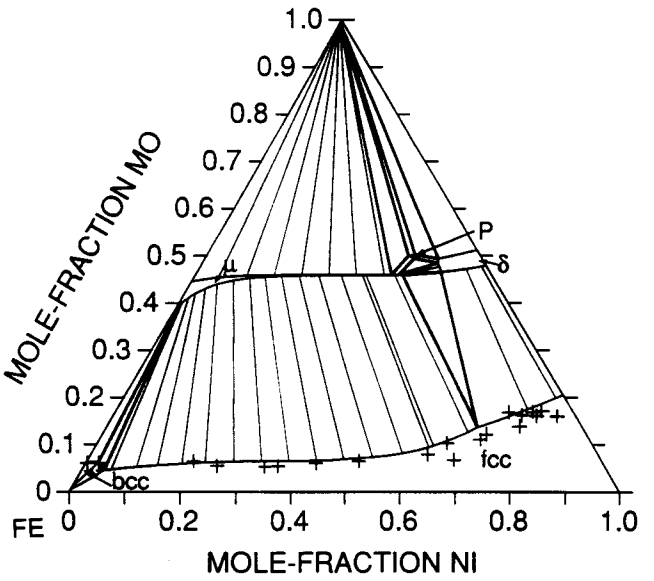

Fig. 13—The calculated isothermal section at 1223 K together with experimental data from the present work. The bcc and fcc phase boundaries were measured by diffusion couple experiments, and the compositions are marked in the diagram as crosses.

agreement with experiments. The isothermal section at 1273 K is shown in Figure 11 and is in good agreement with experimental results from equilibrated alloys from the present work. The calculation is compared with the experimental data by Gan and Jin[9] in Figure 12. The fcc phase boundary is well reproduced by the calculation. However, the three-phase equilibria measured by Gan and Jin are in disagreement, both with the present calculation and with the experimental results of the present work. The isothermal section at 1223 K is plotted in Figure 13. The calculation now predicts a $\mu + P + \delta$ phase equilibrium, found at 1373 K by van Loo *et al.*[8] At this temperature, the experimental results of the present work are reasonably accurate only on the boundaries

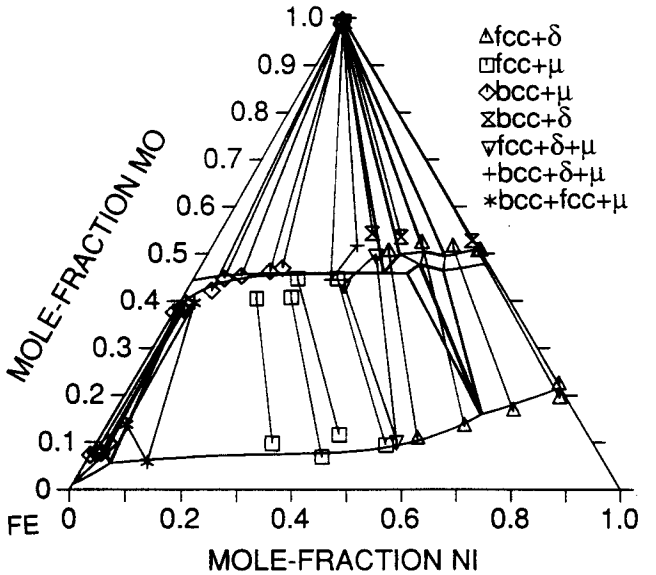

Fig. 12—The calculated isothermal section at 1273 K together with experimental data by Gan and Jin.[9]

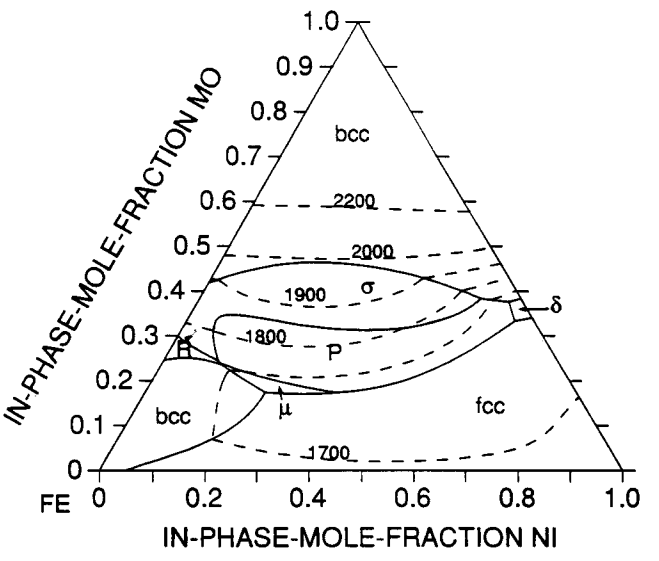

Fig. 14—The calculated projection of the liquidus surfaces of the Fe-Mo-Ni system. The dotted lines are isotherms calculated at every 100 K from 1700 to 2200 K.

of bcc and fcc phase in equilibrium with the intermetallic phases, and these experimental data are well reproduced by the calculation (Figure 13). The experimental data from 1273 and 1223 K were not used for the optimization of the thermodynamic parameters. Still, the agreement between calculations and experiments is good, supporting the present results. The experimental results by Gozlan *et al.*[5] from 1123 and 973 K are in severe disagreement with the results of the present work and with extrapolations from the binary sides and were not further considered.

The calculated projection of the liquidus surface of the Fe-Mo-Ni is shown in Figure 14. The dotted lines are isotherms calculated at every 100 K from 1700 to 2200 K.

VI. SUMMARY

New experimental data in previously unknown regions of the Fe-Mo-Ni system have been obtained using a diffusion couple technique. This technique allows a large number of tie lines to be determined from a reduced number of samples. These data were used for a thermodynamic evaluation of the system. It was shown that it is possible to reproduce most of the experimental data by using relatively simple models. The three-sublattice models adopted for the intermetallic phases can be used to account for the experimental information. Moreover, the thermodynamic analysis was useful in judging experimental data from different sources, for example, experimental data from different temperatures. The thermodynamic description obtained in the present study was determined from experimental data at 1543, 1473, and 1373 K, and it has been shown that experimental data at temperatures below 1373 K can also be described.

APPENDIX

Summary of the thermodynamic parameters evaluated in the present work. For the intermetallic phases, the complete list of parameters is given, and parameters evaluated in the present work are indicated with an asterisk (*). Other parameters are from References 2, 3, 13, and 22. The descriptions of the binary systems are taken from References 2 through 4 and 13. All values are given in SI units. The values are valid for one formula unit of the phases.

The Liquid Phase

1 sublattice, constituents Fe, Mo, Ni

$$* \ {}^{0}L^{\text{Liquid}}_{\text{Fe,Mo,Ni}} = 50{,}000$$

The Bcc Phase

1 sublattice, constituents Fe, Mo, Ni

$$* \ {}^{0}L^{\text{bcc}}_{\text{Fe,Mo,Ni}} = -35{,}743$$

The Fcc Phase

1 sublattice, constituents Fe, Mo, Ni

$$* \ {}^{0}L^{\text{fcc}}_{\text{Fe}} = -204{,}791 + 163.93T$$

$$* \ {}^{0}L^{\text{fcc}}_{\text{Mo}} = +11{,}555 - 55.81T$$

$$* \ {}^{0}L^{\text{fcc}}_{\text{Ni}} = +77{,}975$$

The δ Phase

3 sublattices, sites 24:20:12, constituents Fe, Ni: Fe, Mo, Ni:Mo

$$* \ {}^{\circ}G^{\delta}_{\text{Fe:Fe:Mo}} = +24 \ {}^{\circ}G^{\text{fcc}}_{\text{Fe}} + 20 \ {}^{\circ}G^{\text{bcc}}_{\text{Fe}} + 12 \ {}^{\circ}G^{\text{bcc}}_{\text{Mo}} + 100{,}000$$

$$* \ {}^{\circ}G^{\delta}_{\text{Ni:Fe:Mo}} = +24 \ {}^{\circ}G^{\text{fcc}}_{\text{Ni}} + 20 \ {}^{\circ}G^{\text{bcc}}_{\text{Fe}} + 12 \ {}^{\circ}G^{\text{bcc}}_{\text{Mo}}$$

$$* \ {}^{\circ}G^{\delta}_{\text{Fe:Mo:Mo}} = +24 \ {}^{\circ}G^{\text{fcc}}_{\text{Fe}} + 32 \ {}^{\circ}G^{\text{bcc}}_{\text{Mo}} + 100{,}000$$

$${}^{\circ}G^{\delta}_{\text{Ni:Mo:Mo}} = +24 \ {}^{\circ}G^{\text{fcc}}_{\text{Ni}} + 32 \ {}^{\circ}G^{\text{bcc}}_{\text{Mo}} - 212{,}100 + 1089T - 142T \ln T$$

$$* \ {}^{\circ}G^{\delta}_{\text{Fe:Ni:Mo}} = +24 \ {}^{\circ}G^{\text{fcc}}_{\text{Fe}} + 20 \ {}^{\circ}G^{\text{bcc}}_{\text{Ni}} + 12 \ {}^{\circ}G^{\text{bcc}}_{\text{Mo}}$$

$${}^{\circ}G^{\delta}_{\text{Ni:Ni:Mo}} = +24 \ {}^{\circ}G^{\text{fcc}}_{\text{Ni}} + 20 \ {}^{\circ}G^{\text{bcc}}_{\text{Ni}} + 12 \ {}^{\circ}G^{\text{bcc}}_{\text{Mo}} - 1030 - 93.5T + 13.5T \ln T$$

The μ Phase

3 sublattices, sites 7:2:4, constituents Fe, Ni:Mo: Fe, Mo, Ni

$${}^{\circ}G^{\mu}_{\text{Fe:Mo:Fe}} = +7 \ {}^{\circ}G^{\text{fcc}}_{\text{Fe}} + 2 \ {}^{\circ}G^{\text{bcc}}_{\text{Mo}} + 4 \ {}^{\circ}G^{\text{bcc}}_{\text{Fe}} + 39{,}475 - 6.032T$$

$$* \ {}^{\circ}G^{\mu}_{\text{Ni:Mo:Fe}} = +7 \ {}^{\circ}G^{\text{fcc}}_{\text{Ni}} + 2 \ {}^{\circ}G^{\text{bcc}}_{\text{Mo}} + 4 \ {}^{\circ}G^{\text{bcc}}_{\text{Fe}} + 784{,}294 - 249.607T$$

$${}^{\circ}G^{\mu}_{\text{Fe:Mo:Mo}} = +7 \ {}^{\circ}G^{\text{fcc}}_{\text{Fe}} + 6 \ {}^{\circ}G^{\text{bcc}}_{\text{Mo}} - 46{,}663 - 5.891T$$

$$* \ {}^{\circ}G^{\mu}_{\text{Ni:Mo:Mo}} = +7 \ {}^{\circ}G^{\text{fcc}}_{\text{Ni}} + 6 \ {}^{\circ}G^{\text{bcc}}_{\text{Mo}} + 28{,}506 - 47.3T$$

$$* \ {}^{\circ}G^{\mu}_{\text{Fe:Mo:Ni}} = +7 \ {}^{\circ}G^{\text{fcc}}_{\text{Fe}} + 2 \ {}^{\circ}G^{\text{bcc}}_{\text{Mo}} + 4 \ {}^{\circ}G^{\text{bcc}}_{\text{Ni}} + 354{,}030 - 229.4T$$

$$* \ {}^{\circ}G^{\mu}_{\text{Ni:Mo:Ni}} = +7 \ {}^{\circ}G^{\text{fcc}}_{\text{Ni}} + 2 \ {}^{\circ}G^{\text{bcc}}_{\text{Mo}} + 4 \ {}^{\circ}G^{\text{bcc}}_{\text{Ni}} + 398{,}566 - 200T$$

The P Phase

3 sublattices, sites 24:20:12, constituents Fe, Ni: Fe, Mo, Ni:Mo

$$* \ {}^{\circ}G^{P}_{\text{Fe:Fe:Mo}} = +24 \ {}^{\circ}G^{\text{fcc}}_{\text{Fe}} + 20 \ {}^{\circ}G^{\text{bcc}}_{\text{Fe}} + 12 \ {}^{\circ}G^{\text{bcc}}_{\text{Mo}} + 111{,}361$$

$$* \ {}^{\circ}G^{P}_{\text{Ni:Fe:Mo}} = +24 \ {}^{\circ}G^{\text{fcc}}_{\text{Ni}} + 20 \ {}^{\circ}G^{\text{bcc}}_{\text{Fe}} + 12 \ {}^{\circ}G^{\text{bcc}}_{\text{Mo}} - 170{,}245 + 100T$$

$$* \ {}^{\circ}G^{P}_{\text{Fe:Mo:Mo}} = +24 \ {}^{\circ}G^{\text{fcc}}_{\text{Fe}} + 32 \ {}^{\circ}G^{\text{bcc}}_{\text{Mo}} + 362{,}525 - 332.7T$$

$$* {}^{\circ}G^{p}_{Ni:Mo:Mo} = +24\,{}^{\circ}G^{fcc}_{Ni} + 32\,{}^{\circ}G^{bcc}_{Mo} + 26{,}739 - 100T$$

$$* {}^{\circ}G^{p}_{Fe:Ni:Mo} = +24\,{}^{\circ}G^{fcc}_{Fe} + 20\,{}^{\circ}G^{bcc}_{Ni} + 12\,{}^{\circ}G^{bcc}_{Mo}$$

$$* {}^{\circ}G^{p}_{Ni:Ni:Mo} = +24\,{}^{\circ}G^{fcc}_{Ni} + 20\,{}^{\circ}G^{bcc}_{Ni} + 12\,{}^{\circ}G^{bcc}_{Mo} + 208{,}845 - 100T$$

The R Phase

3 sublattices, sites 27:14:12, constituents Fe, Ni: Mo:Fe, Mo, Ni

$${}^{\circ}G^{R}_{Fe:Mo:Fe} = +27\,{}^{\circ}G^{fcc}_{Fe} + 14\,{}^{\circ}G^{bcc}_{Mo} + 12\,{}^{\circ}G^{bcc}_{Fe} - 77{,}487 - 50.486T$$

$$* {}^{\circ}G^{R}_{Ni:Mo:Fe} = +27\,{}^{\circ}G^{fcc}_{Ni} + 14\,{}^{\circ}G^{bcc}_{Mo} + 12\,{}^{\circ}G^{bcc}_{Fe}$$

$${}^{\circ}G^{R}_{Fe:Mo:Mo} = +27\,{}^{\circ}G^{fcc}_{Fe} + 26\,{}^{\circ}G^{bcc}_{Mo} + 313{,}474 - 289.472T$$

$$* {}^{\circ}G^{R}_{Ni:Mo:Mo} = +27\,{}^{\circ}G^{fcc}_{Ni} + 26\,{}^{\circ}G^{bcc}_{Mo} - 18{,}000$$

$$* {}^{\circ}G^{R}_{Fe:Mo:Ni} = +27\,{}^{\circ}G^{fcc}_{Fe} + 14\,{}^{\circ}G^{bcc}_{Mo} + 12\,{}^{\circ}G^{bcc}_{Ni}$$

$$* {}^{\circ}G^{R}_{Ni:Mo:Ni} = +27\,{}^{\circ}G^{fcc}_{Ni} + 14\,{}^{\circ}G^{bcc}_{Mo} + 12\,{}^{\circ}G^{bcc}_{Ni} + 100{,}000$$

The σ Phase

3 sublattices, sites 8:18:4, constituents Fe, Ni: Fe, Mo, Ni:Mo

$${}^{\circ}G^{\sigma}_{Fe:Fe:Mo} = +8\,{}^{\circ}G^{fcc}_{Fe} + 18\,{}^{\circ}G^{bcc}_{Fe} + 4\,{}^{\circ}G^{bcc}_{Mo} - 1813 - 27.272T$$

$$* {}^{\circ}G^{\sigma}_{Ni:Fe:Mo} = +8\,{}^{\circ}G^{fcc}_{Ni} + 18\,{}^{\circ}G^{bcc}_{Fe} + 4\,{}^{\circ}G^{bcc}_{Mo} + 658{,}600 - 200T$$

$${}^{\circ}G^{\sigma}_{Fe:Mo:Mo} = +8\,{}^{\circ}G^{fcc}_{Fe} + 22\,{}^{\circ}G^{bcc}_{Mo} + 83{,}326 - 69.618T$$

$${}^{\circ}G^{\sigma}_{Ni:Mo:Mo} = +8\,{}^{\circ}G^{fcc}_{Ni} + 22\,{}^{\circ}G^{bcc}_{Mo} + 85{,}662$$

$$* {}^{\circ}G^{\sigma}_{Fe:Ni:Mo} = +8\,{}^{\circ}G^{fcc}_{Fe} + 18\,{}^{\circ}G^{bcc}_{Ni} + 4\,{}^{\circ}G^{bcc}_{Mo} + 408{,}600 - 200T$$

$${}^{\circ}G^{\sigma}_{Ni:Ni:Mo} = +8\,{}^{\circ}G^{fcc}_{Ni} + 18\,{}^{\circ}G^{bcc}_{Ni} + 4\,{}^{\circ}G^{bcc}_{Mo} - 16{,}385$$

$${}^{0}L^{\sigma}_{Fe:Fe,Mo:Mo} = +222{,}909$$

$$* {}^{0}L^{\sigma}_{Fe,Ni:Mo:Mo} = -164{,}570 - 10T$$

ACKNOWLEDGMENTS

I wish to thank Professor M. Hillert for useful advice, constructive criticism, and help received during the preparation of this article. I also wish to thank Nils Lange for the help with the experimental work. The alloys used in this study were supplied by Sandvik AB. All diagrams were calculated using the THERMO-CALC databank developed by Drs. Bo Sundman, Bo Jansson, and Jan-Olof Andersson at the Division of Physical Metallurgy,[24] and the optimizations were performed using the computer program PARROT developed by Dr. Bo Jansson.[25]

REFERENCES

1. G.V. Raynor and V.G. Rivlin: *Int. Met. Rev.*, 1984, vol. 29, pp. 329-75.
2. A. Fernández Guillermet: Consejo National de Investigationes Cientificas y Tecnicas, Centro Atomico Bariloche, San Carlos de Bariloche, Argentina, personal communication, 1984.
3. K. Frisk: *CALPHAD*, 1990, vol. 14 (3), pp. 311-20.
4. Zhong Shu Xing, D.D. Gohil, A.T. Dinsdale, and T.G. Chart: DMA(A)103, Report National Physics Laboratory, London, 1985.
5. E. Gozlan, M. Bamberger, S.F. Dirnfeld, B. Prinz, and J. Klodt: *Mat. Sci. Eng.*, 1990, vol. A141, pp. 85-95.
6. W. Köster: *Arch. Eisenhuettenwes.*, 1934, vol. 8, pp. 169-71.
7. D.K. Das, S.P. Rideout, and P.A. Beck: *J. Met.*, 1952, vol. 4, pp. 1071-75.
8. F.J.J. van Loo, G.F. Bastin, J.W.G.A. Vrolijk, and J.J.M. Hendriks: *J. Less-Common Met.*, 1980, vol. 72, pp. 225-30.
9. W. Gan and Z. Jin: *J. Less-Common Met.*, 1990, vol. 160, pp. 29-33.
10. A. Fernández Guillermet and P. Gustafson: *High-Temp.-High Pressures*, 1984, vol. 16, pp. 591-610.
11. A. Fernández Guillermet: *Int. J. Thermophys.*, 1985, vol. 6, pp. 367-93.
12. A.T. Dinsdale: Report DMA(A)195, National Physics Laboratory, London, 1989.
13. A. Fernández Guillermet: *Bull. Alloy Phase Diagrams*, 1982, vol. 3 (3), pp. 359-84.
14. M. Hillert and L.-I. Staffansson: *Acta Chem. Scand.*, 1970, vol. 24, pp. 3618-26.
15. B. Sundman and J. Ågren: *J. Phys. Chem. Solids*, 1981, vol. 42, pp. 297-301.
16. A. Fernández Guillermet and L. Östlund: *Metall. Trans. A*, 1986, vol. 17A, pp. 1809-23.
17. P. Gustafson: *Metall. Trans. A*, 1988, vol. 19A, pp. 2531-46.
18. J.-O. Andersson and N. Lange: *Metall. Trans. A*, 1988, vol. 19A, pp. 1385-94.
19. P. Gustafson: *Z. Metallkd.*, 1988, vol. 79, pp. 388-96.
20. A.K. Sinha: *Prog. Mater. Sci.*, 1972, vol. 15, pp. 81-179.
21. S.R. Rideout, W.D. Manly, L.E. Kamen, B.S. Lement, and P.A. Beck: *Trans. AIME*, 1951, vol. 191, pp. 872-76.
22. K. Frisk: Trita-Mac-0429, Division of Physical Metallurgy, Royal Institute of Technology, Stockholm, 1990.
23. J.-O. Andersson, A. Fernández Guillermet, M. Hillert, B. Jansson, and B. Sundman: *Acta Metall.*, 1986, vol. 34, pp. 437-45.
24. B. Sundman, B. Jansson, and J.-O. Andersson: *CALPHAD*, 1985, vol. 9, pp. 153-90.
25. B. Jansson: Ph.D. Thesis, The Royal Institute of Technology, Stockholm, 1984.
26. M. Bamberger, S.F. Dirnfeld, E. Gozlan, J. Klodt, B. Prinz, J.A. Golczewski, and H.L. Lukas: Technion, Israel Institute of Technology, Haifa, Israel, unpublished research, 1989.